IEMS Vol. 7, No. 2, pp. 101-112, September 2008.

A Synthetic Exponentially Weighted Moving-average Chart for High-yield Processes

Etsuko Kusukawa†
Department of Electrical Engineering and Information Systems
Osaka Prefecture University, Sakai, Osaka, 599-8531, JAPAN
Tel: +81-72-254-9349, Fax: +81-72-254-9915, E-mail: kusukawa@eis.osakafu-u.ac.jp

Takayuki Kotani
Department of Industrial Engineering
Osaka Prefecture University, Sakai, Osaka, 599-8531, JAPAN
Tel: +81-72-254-9349, Fax: +81-72-254-9915, E-mail: kusukawa@eis.osakafu-u.ac.jp

Hiroshi Ohta
Department of Industrial Engineering
Osaka Prefecture University, Sakai, Osaka, 599-8531, JAPAN
Tel: +81-72-254-9349, Fax: +81-72-254-9915, E-mail: kusukawa@eis.osakafu-u.ac.jp

Selected paper from APIEM 2006

Abstract. As charts to monitor the process fraction defectives, P, in the high-yield processes, Mishima *et al.* (2002) discussed a synthetic chart, the Synthetic CS chart, which integrates the CS (Confirmation Sample)$_{\text{CCC (Cumulative Count of Conforming)-}r}$ chart and the CCC-r chart. The Synthetic CS chart is designed to monitor quality characteristics in real-time. Recently, Kotani *et al.* (2005) presented the EWMA (Exponentially Weighted Moving-Average)$_{\text{CCC-}r}$ chart, which considers combining the quality characteristics monitored in the past with one monitored in real-time. In this paper, we present an alternative chart that is more superior to the EWMA$_{\text{CCC-}r}$ chart. It is an integration of the EWMA$_{\text{CCC-}r}$ chart and the CCC-r chart. In using the proposed chart, the quality characteristic is initially judged as either the in-control state or the out-of-control state, using the lower and upper control limits of the EWMA$_{\text{CCC-}r}$ chart. If the process is not judged as the in-control state by the EWMA$_{\text{CCC-}r}$ chart, the process is successively judged, using the CCC-r chart to confirm the judgement of the EWMA$_{\text{CCC-}r}$ chart. We compare the ANOS (Average Number of Observations to Signal) of the proposed chart with those of the EWMA$_{\text{CCC-}r}$ chart and the Synthetic CS chart. From the numerical experiments, with the small size of inspection items, the proposed chart is the most sensitive to detect especially the small shifts in P among other charts.

Keywords: High-yield process, Synthetic chart, EWMA (Exponentially Weighted Moving-average) chart, CCC (Cumulative Count of Conforming)-r chart, ANOS (Average Number of Observations to Signal), Markov chain approach

1. INTRODUCTION

Recently, it is well known that the traditional Shewhart-type charts do not respond sensitively to the small or moderate shifts in quality characteristics obtained from the process (See Montgomery 2001). Roberts (1959, 1966) presented the EWMA (Exponentially Weighted Moving Average) chart to detect the small shifts in the process mean as an alternative of the Shewhart $\bar{x}$ chart. Many other EWMA charts for variables have been proposed for recent years (See Crowder, 1987; Ng and Case, 1989; Lucas and Saccucci, 1990, Domangue and Patch, 1991, Reynolds, 1996 and Steiner, 1998). As the EWMA chart for attributes, Gan (2002) and Borror *et al.* (1998) presented the EWMA chart to monitor the count of defects which follows the Poisson distribution, referred to as the EWMAc chart, as an alternative Shewhart c chart. The Markov chain approach is used to calculate the Average

† : Corresponding Author

Run Length (ARL).

On the other hand, the manufacturing processes, especially in the electronic industries, have been automated with the aid of computers and the modern technologies. The items are produced and checked one by one (See Xie *et al*., 1998). Moreover, in the high-yield processes seen in the manufacturing environment of today, the process fraction defectives P is substantially less than one percent. Few or even no items are nonconforming even for a fairly large sample. As one effective way, Xie *et al*. (1998) presented an alternative chart to monitor the process fraction defectives P for the high-yield processes, referred to as the CCC (Cumulative Count of Conforming)-r chart. The quality characteristic is the cumulative count of item inspected until observing $r(\geq 2)$ nonconforming items. Furthermore, as an alternative of the CCC-r chart, Ohta and Kusukawa (2004) presented the CS (Confirmation Sample)$_{\text{CCC-}r}$ chart by applying the CS charting procedure proposed by Steiner (1999) to the CCC-r chart. It is illustrated that the CS $_{\text{CCC-}r}$ chart is more sensitive than the CCC-r chart to detect the small or moderate shifts in P to both the upward and downward directions, which indicate the process deterioration and the process improvement, respectively. In order to enhance the performance of the $\text{CS}_{\text{CCC-}r}$ chart, Mishima *et al.* (2002) presented a synthetic chart which integrates the $\text{CS}_{\text{CCC-}r}$ chart and the CCC-r chart, referred to as the Synthetic CS chart. The Synthetic CS chart has the higher detection powers for the small or moderate shifts in P than the $\text{CS}_{\text{CCC-}r}$ chart. However, above charts are designed to monitor quality characteristics in real-time. Neither the $\text{CS}_{\text{CCC-}r}$ chart nor the Synthetic CS chart has the detection power required for the small or moderate shifts in P.

Recently, Kotani *et al.* (2005) presented the EWMA (Exponentially Weighted Moving-Average)$_{\text{CCC-}r}$ chart, which considers combining the quality characteristics monitored in the past with one monitored in real-time. The $\text{EWMA}_{\text{CCC-}r}$ chart is constructed by applying the designing method of the EWMA chart for attributes (See Montgomery, 2001; Gan, 2002; Borror *et al*., 1998) to the CCC-r chart. The $\text{EWMA}_{\text{CCC-}r}$ chart has the higher detection powers for any shifts in P than the $\text{CS}_{\text{CCC-}r}$ chart.

In the real field, the fundamental aim of the monitoring and improving actions of the process quality is always to realize the zero-defects processes. From this viewpoint, in this paper, we focus on enhancing the detention power for especially the small shifts in P to both the upward and downward directions which the process deterioration and the process improvement in the high-yield processes. Concretely, as a more superior chart to the $\text{EWMA}_{\text{CCC-}r}$ chart and the Synthetic CS chart, we present a synthetic chart that is an integration of the $\text{EWMA}_{\text{CCC-}r}$ chart and the CCC-r chart. In what follows, the proposed chart is referred to as the Synthetic EWMA chart. In using the Synthetic EWMA chart, the quality characteristic is initially judged as either the in-control state or the out-of-control state, using the lower and upper control limits of the $\text{EWMA}_{\text{CCC-}r}$ chart. If the process is not judged as the in-control state by the $\text{EWMA}_{\text{CCC-}r}$ chart, the process is successively judged, using the CCC-r chart to confirm the judgement of the $\text{EWMA}_{\text{CCC-}r}$ chart.

In order to assess the performance of the detection power of the Synthetic EWMA chart, we compare the ANOS (Average Number of Observations to Signal) of the Synthetic EWMA chart with those of both the stand-alone $\text{EWMA}_{\text{CCC-}r}$ chart and the Synthetic CS chart.

Each ANOS of the stand-alone $\text{EWMA}_{\text{CCC-}r}$ chart and the Synthetic EWMA chart can be obtained based on the Markov chain approach discussed by Borror *et al.* (1998). Concretely, for the stand-alone $\text{EWMA}_{\text{CCC-}r}$ chart, the Markov chain approach is used to calculate the ANOS based on the designing method of the EWMA_{C} chart. For the Synthetic EWMA chart, the Markov chain approach is used to calculate the ANOS based on the designing method of the $\text{EWMA}_{\text{CCC-}r}$ chart. From the numerical experiments, with the small size of inspection items, the Synthetic EWMA chart is the most sensitive to detect especially small shifts in P from the in-control state to both the upward and downward directions in the high-yield processes among the stand-alone $\text{EWMA}_{\text{CCC-}r}$ chart and the Synthetic CS chart. The proposed process monitoring technique can be implemented by the on-line computers and the modern inspection equipment in the automated manufacturing environments in order to enhance the detection power for the small shifts in P.

2. NOTATION

P : the process fraction defectives.

P_0: the in-control process fraction defectives.

P_1: the out-of-control process fraction defectives.

α : the specified value of the overall probability of type I error for the stand-alone CCC-r chart, the stand-alone $\text{CS}_{\text{CCC-}r}$ chart, the stand-alone $\text{EWMA}_{\text{CCC-}r}$ chart, the Synthetic CS chart and the Synthetic EWMA chart.

α_{CS} : the specified value of the probability of type I error for the $\text{CS}_{\text{CCC-}r}$ chart in the Synthetic CS chart.

$\alpha^{\text{CS}}_{\text{CCC-}r}$: the specified value of the probability of type I error for the CCC-r chart in the Synthetic CS chart.

α_{EWMA} : the specified value of the probability of type I error for the $\text{EWMA}_{\text{CCC-}r}$ chart in the Synthetic EWMA chart.

$\alpha^{\text{EWMA}}_{\text{CCC-}r}$: the specified value of the probability of type I error for the CCC-r chart in the Synthetic EWMA chart.

$r_z\,(z \in \text{CCC-}r, \text{CS}, \text{EWMA})$: the number of nonconforming item observed before a point is plotted on the following chart: the CCC-r chart, the $\text{CS}_{\text{CCC-}r}$ chart and the $\text{EWMA}_{\text{CCC-}r}$ chart used in either the stand-alone chart or the Synthetic

chart (The recommended value is about 2-5 depending on the process fraction defectives and type of process being monitored (See Xie *et al.*, 1998)).

$x_z\,(z \in \text{CCC-}r, \text{CS})$: quality characteristic observed from the process which follows each negative binomial distribution $NB(r_z, P)$ $(z \in \text{CCC-}r, \text{CS})$ to monitor on the stand-alone CCC-*r* chart or both the stand-alone $CS_{CCC\text{-}r}$ chart and the $CS_{CCC\text{-}r}$ chart in the Synthetic CS chart.

x_t : the *t* th quality characteristic based on the cumulative count of item inspected until observing r_{EWMA} nonconforming items from the process which follows the negative binomial distribution *NB* (r_{EWMA}, *P*).

x_A: the first quality characteristic of both the stand-alone $CS_{CCC\text{-}r}$ chart and the $CS_{CCC\text{-}r}$ chart in the Synthetic CS chart based on the cumulative count of item inspected until observing r_{CS} nonconforming items from the process which follows the negative binomial distribution *NB* (r_{CS}, *P*).

x_B: the second quality characteristic for confirmation of both the stand-alone $CS_{CCC\text{-}r}$ chart and the $CS_{CCC\text{-}r}$ chart in the Synthetic CS chart based on the cumulative count of item inspected until observing r_{CS} nonconforming items from the process which follows the negative binomial distribution *NB* (r_{CS}, *P*).

$LCSL_{CS}$: the lower confirmation control limit of the stand-alone $CS_{CCC\text{-}r}$ chart.

$UCSL_{CS}$: the upper confirmation control limit of the stand-alone $CS_{CCC\text{-}r}$ chart.

LCSLs: the lower confirmation control limit of the $CS_{CCC\text{-}r}$ chart in the Synthetic CS chart.

UCSLs: the upper confirmation control limit of the $CS_{CCC\text{-}r}$ chart in the Synthetic CS chart.

Q_{LCSLs}: the lower type I error of the $CS_{CCC\text{-}r}$ chart in the Synthetic CS chart.

Q_{UCSLs}: the upper type I error of the $CS_{CCC\text{-}r}$ chart in the Synthetic CS chart.

N_{LCSLs}: the cumulative count of x_A inspected until observing $r_{CCC\text{-}r}$ nonconforming quality characteristics that both x_A and x_B exceed the lower confirmation control limit of the $CS_{CCC\text{-}r}$ chart in the Synthetic CS chart.

N_{UCSLs}: the cumulative count of x_A inspected until observing $r_{CCC\text{-}r}$ nonconforming quality characteristics that both x_A and x_B exceed the upper confirmation control limit of the $CS_{CCC\text{-}r}$ chart in the Synthetic CS chart.

LCL_{LCSLs}: the lower control limit of the CCC-*r* chart in the Synthetic CS chart used in the second judgment of the process state for the lower detection on the $CS_{CCC\text{-}r}$ chart which detects changes to lower shift in P_0 indicating the process improvement.

LCL_{UCSLs}: the lower control limit of the CCC-*r* chart in the Synthetic CS chart used in the second judgment of the process state for the upper detection on the $CS_{CCC\text{-}r}$ chart which detects changes to upper shift in P_0 indicating the process deterioration.

Z_t: the *t* th plotting point of the stand-alone $EWMA_{CCC\text{-}r}$ chart.

h_L: the lower control limit of the stand-alone $EWMA_{CCC\text{-}r}$ chart.

h_U: the upper control limit of the stand-alone $EWMA_{CCC\text{-}r}$ chart.

Z_t^S : the *t* th plotting point of the $EWMA_{CCC\text{-}r}$ chart in the Synthetic EWMA chart.

h_L^S : the lower control limit of the $EWMA_{CCC\text{-}r}$ chart in the Synthetic EWMA chart.

h_U^S : the upper control limit of the $EWMA_{CCC\text{-}r}$ chart in the Synthetic EWMA chart.

N_{EWMA}: the cumulative count of Z_t^S plotted on the $EWMA_{CCC\text{-}r}$ chart in the Synthetic EWMA chart until observing $r_{CCC\text{-}r}\,(\geq 2)$ nonconforming quality characteristics that Z_t^S exceeds the upper or lower control limit of the $EWMA_{CCC\text{-}r}$ chart in the Synthetic EWMA chart.

LCL: the lower control limit of the CCC-*r* chart in the Synthetic EWMA chart.

3. OUTLINE OF THE STAND-ALONE CCC-*r* CHART

The quality characteristic of the stand-alone CCC-*r* chart, $x_{CCC\text{-}r}$, is defined as the cumulative count of item inspected until observing $r_{CCC\text{-}r}$ ($\geq$ 2) nonconforming items. When the overall probability of type I error is specified as α , the stand-alone CCC-*r* chart can be designed by using the probability limit method based on the negative binomial distribution with parameters $r_{CCC\text{-}r}$ and P_0. The lower and upper control limits of the stand-alone CCC-*r* chart, denoted as $LCL_{CCC\text{-}r}$ and $UCL_{CCC\text{-}r}$, are obtained respectively as the solutions of the following equations:

$$\sum_{i=r_{CCC\text{-}r}}^{LCL_{CCC\text{-}r}} \binom{i-1}{r_{CCC\text{-}r}-1} P_0^{r_{CCC\text{-}r}} (1-P_0)^{i-r_{CCC\text{-}r}} = \alpha/2\,, \quad (1)$$

$$\sum_{i=r_{CCC\text{-}r}}^{UCL_{CCC\text{-}r}} \binom{i-1}{r_{CCC\text{-}r}-1} P_0^{r_{CCC\text{-}r}} (1-P_0)^{i-r_{CCC\text{-}r}} = 1-\alpha/2 \quad (2)$$

(See Xie *et al.*, 1998). As $r_{CCC\text{-}r}$ is getting larger, the stand-alone CCC-*r* chart is more and more sensitive to detect the small or moderate shifts in *P* to the upward direction, while the stand-alone CCC-*r* chart needs more and more observations to obtain a plotting point on the chart, then the cost is fairly high. The decision procedure in the stand-alone CCC-*r* chart is made as follows: in the stand-alone CCC-*r* chart, if *P* decreases as like $P < P_0$, then the quality characteristic of the stand-alone CCC-*r* chart is expected to be larger, while if *P* increases as like $P > P_0$, then it is expected to be smaller. Therefore, according to the stand-alone CCC-*r* chart, if a plotted point is above the upper control limit, the proc-

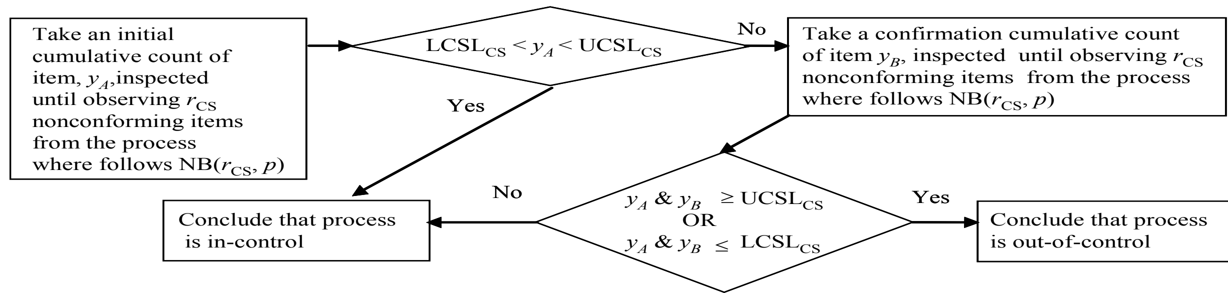

Figure 1. Decision procedure of the stand-alone $CS_{CCC\text{-}r}$ Chart.

ess is likely to have improved, while if a plotted point is below the lower control limit, the process has probably deteriorated.

4. OUTLINE OF THE STAND-ALONE $CS_{CCC\text{-}r}$ CHART

Figure 1 shows the decision procedure of the stand-alone $CS_{CCC\text{-}r}$ chart proposed by Ohta and Kusukawa (2004). In the stand-alone $CS_{CCC\text{-}r}$ chart, x_A is initially taken from the process. Then x_A is judged whether the process is in-control or out-of- control, using the lower and upper confirmation control limits of the stand-alone $CS_{CCC\text{-}r}$ chart, $LCSL_{CS}$ and $UCSL_{CS}$, respectively. If x_A satisfies the following condition:

$$LCSL_{CS} < x_A < UCSL_{CS}\,, \tag{3}$$

it would be judged that the process is in-control. On the other hand, if x_A satisfies the following condition:

$$x_A \le LCSL_{CS} \text{ OR } UCSL_{CS} \le x_A\,, \tag{4}$$

the second quality characteristic for confirmation, x_B, would be independently taken from the same process. Furthermore, the initial quality characteristic x_A and the confirmation quality characteristic x_B would be judged whether the process is in-control or out-of-control, using the same confirmation control limits. If both x_A and x_B, denoted as x_A & x_B, satisfy the following condition:

$$x_A \,\&\, x_B \le LCSL_{CS} \text{ OR } UCSL_{CS} \le x_A \,\&\, x_B, \tag{5}$$

it would be judged that the process is out-of-control. On the other hand, if both x_A and x_B do not satisfy equation (5), it would be judged that the process is in-control. The overall probability of the type I error assuming the fixed values for the confirmation control limits, α , can be obtained as follows:

$$\begin{aligned}\alpha &= P(x_A \& x_B \ge UCSL_{CS}) + P(x_A \& x_B \le LCSL_{CS}) \\ &= P(x_{CS} \ge UCSL_{CS})^2 + P(x_{CS} \le LCSL_{CS})^2.\end{aligned} \tag{6}$$

In this paper, it is assumed that type I error in either direction is equally undesirable. From equation (6), the lower and upper confirmation control limits of the stand-alone $CS_{CCC\text{-}r}$ chart, denoted as $LCSL_{CS}$ and $UCSL_{CS}$, can be obtained as the solutions of the following equations:

$$\sum_{i=r_{CS}}^{LCSL_{CS}} \binom{i-1}{r-1} P_0^{r_{CS}} (1-P_0)^{i-r_{CS}} = \sqrt{\alpha/2}\,, \tag{7}$$

$$\sum_{i=r_{CS}}^{UCSL_{CS}} \binom{i-1}{r-1} P_0^{r_{CS}} (1-P_0)^{i-r_{CS}} = 1-\sqrt{\alpha/2}\,. \tag{8}$$

5. OUTLINE OF THE SYNTHETIC CS CHART

5.1 Decision Procedure of the Synthetic CS Chart for The Process

The decision procedure of the Synthetic CS chart proposed by Mishima *et al.* (2002) is shown as follows:

Step 1: For the $CS_{CCC\text{-}r}$ chart in the Synthetic CS chart, x_A is initially taken from the process.

Step 2: If x_A exceeds either the lower conformation control limit or the upper conformation control limit of the $CS_{CCC\text{-}r}$ chart in the Synthetic CS chart, the second independent quality characteristic for confirmation, x_B, would be taken from the same process.

Step 3: If both x_A and x_B exceed the same side confirmation control limit of the $CS_{CCC\text{-}r}$ chart in the Synthetic CS chart, the process is furthermore successively judged, using the CCC-*r* chart in the Synthetic CS chart.

Step 4: For the CCC-*r* chart in the Synthetic CS chart, both x_A and x_B that exceed the same side confirmation control limit of the $CS_{CCC\text{-}r}$ chart in the Synthetic CS chart is counted as one nonconforming item of the CCC-*r* chart in the Synthetic CS chart.

Step 5: For shifts in the process fraction defectives, P, from the in-control state to the upward direction, N_{UCSLs} is observed until both x_A and x_B exceed

the upper confirmation control limit of the $CS_{CCC\text{-}r}$ chart in the Synthetic CS chart.

Step 6: For shifts in the process fraction defectives, P, from the in-control state to downward direction, N_{LCSLs} is observed until both x_A and x_B exceed the lower confirmation control limit of the $CS_{CCC\text{-}r}$ chart in the Synthetic CS chart.

Step 7: If either N_{UCSLs} or N_{LCSLs} exceeds each of the lower control limits of the CCC-r chart in the Synthetic CS chart setting for N_{UCSLs} or N_{LCSLs}, it would be judged that the process is out-of-control. Otherwise, it would be judged that the process is in-control.

5.2 Settings of Type I Error and The Control Limits of the Synthetic CS Chart

The lower and upper confirmation control limits of the $CS_{CCC\text{-}r}$ chart in the Synthetic CS chart can be designed based on the negative binomial distribution NB (r_{CS}, P). As with equation (6), the probability of type I error, α_{CS}, of the $CS_{CCC\text{-}r}$ chart in the Synthetic CS chart can be obtained as

$$\begin{aligned}\alpha_{CS} &= P(x_A \& x_B \geq \text{UCSLs}) + P(x_A \& x_B \leq \text{LCSLs}) \\ &= P(x_{CS} \geq \text{UCSLs})^2 + P(x_{CS} \leq \text{LCSLs})^2. \quad (9)\end{aligned}$$

From equation (9), using the probability limit method based on the negative binomial distribution, the lower and upper confirmation control limits, denoted as LCSLs and UCSLs, of the $CS_{CCC\text{-}r}$ chart in the Synthetic CS chart can be obtained as the solutions of the following equations:

$$\sum_{i=r_{CS}}^{\text{LCSLs}} \binom{i-1}{r_{CS}-1} P_0^{r_{CS}} (1-P_0)^{i-r_{CS}} = \sqrt{\alpha_{CS}/2}\,, \quad (10)$$

$$\sum_{i=r_{CS}}^{\text{UCSLs}} \binom{i-1}{r_{CS}-1} P_0^{r_{CS}} (1-P_0)^{i-r_{CS}} = 1-\sqrt{\alpha_{CS}/2}\,. \quad (11)$$

The CCC-r chart in the Synthetic CS chart can be designed based on the probabilities of the lower and upper type I errors for the $CS_{CCC\text{-}r}$ chart in the Synthetic CS chart. Here, the lower and upper type I errors of the $CS_{CCC\text{-}r}$ chart in the Synthetic CS chart, denoted as Q_{LCSLs} and Q_{UCSLs}, can be obtained as the solutions of the following equations:

$$Q_{\text{LCSL}_s} = \left[\sum_{i=r_{CS}}^{\text{LCSL}_s} \binom{i-1}{r_{CS}-1} P_0^{r_{CS}} (1-P_0)^{i-r_{CS}}\right]^2, \quad (12)$$

$$Q_{\text{UCSL}_s} = \left[1-\sum_{i=r_{CS}}^{\text{UCSL}_s} \binom{i-1}{r_{CS}-1} P_0^{r_{CS}} (1-P_0)^{i-r_{CS}}\right]^2. \quad (13)$$

When the probability of type I error is specified as α_{CCC-r}^{CS} for the CCC-r chart in the Synthetic CS chart, the lower control limit of the CCC-r chart in the Synthetic CS chart for the lower detection of the $CS_{CCC\text{-}r}$ chart in the Synthetic CS chart, LCL_{LCSLs}, can be obtained as

$$\sum_{i=r_{CCC-r}}^{\text{LCL}_{\text{LCSL}_s}} \binom{i-1}{r_{CCC-r}-1} Q_{\text{LCSL}_s}^{r_{CCC-r}} (1-Q_{\text{LCSL}_s})^{i-r_{CCC-r}} = \alpha_{CCC-r}^{CS}\,. \quad (14)$$

The lower control limit of the CCC-r chart in the Synthetic CS chart for the upper detection of the $CS_{CCC\text{-}r}$ chart in the Synthetic CS chart, LCL_{UCSLs}, can be obtained as

$$\sum_{i=r_{CCC-r}}^{\text{LCL}_{\text{UCSL}_s}} \binom{i-1}{r_{CCC-r}-1} Q_{\text{UCSL}_s}^{r_{CCC-r}} (1-Q_{\text{UCSL}_s})^{i-r_{CCC-r}} = \alpha_{CCC-r}^{CS}\,. \quad (15)$$

The overall probability of type I error for the Synthetic CS chart, α, can be obtained as

$$\begin{aligned}\alpha &= P(x_{CS} \geq \text{UCSLs})^2 P(N_{UCSLs} \leq LCL_{UCSLs}) \\ &\quad + P(x_{CS} \leq \text{LCSLs})^2 P(N_{LCSLs} \leq LCL_{LCSLs}) \\ &= \alpha_{CS} \times \alpha_{CCC-r}^{CS}\,. \quad (16)\end{aligned}$$

It is revealed from the numerical experiments for the Synthetic CS chart investigated by Kusukawa and Ohta (2003) that the Synthetic CS chart is the most sensitive to detect any shifts in quality characteristics when the Synthetic CS chart is designed by the set values of type I error as

$$\alpha_{CS} = \alpha_{CCC-r}^{CS} = \sqrt{\alpha}\,. \quad (17)$$

6. OUTLINE OF THE STAND-ALONE $EWMA_{CCC\text{-}r}$ CHART

The stand-alone $EWMA_{CCC\text{-}r}$ chart proposed by Kotani *et al.* (2005) can be constructed by applying the designing method of the stand-alone EWMA chart for attributes (See Montgomery, 2001; Gan, 2002; Borror *et al.*, 1998) to the CCC-r chart. Using the t th cumulative count x_t of item inspected until observing r_{EWMA} nonconforming items on the process, a plotting point of the stand-alone $EWMA_{CCC\text{-}r}$ chart is obtained by

$$Z_t = \lambda x_t + (1-\lambda) Z_{t-1} \; (0 < \lambda \leq 1,\; t = 1, 2 \cdots), \quad (18)$$

where λ is a smoothing constant such that $0 < \lambda \leq 1$. When the process is the in-control state with the fraction defectives P_0, it assumes that the process obeys the negative binomial distribution NB(r_{EWMA}, P_0). Under the situation, mean and variance of the cumulative count x are

$$E[x]=\frac{r_{\mathrm{EWMA}}}{P_0} \quad \text{and} \quad V[x]=\frac{r_{\mathrm{EWMA}}(1-P_0)}{P_0^2}, \quad (19)$$

For a plotting point Z_t of the EWMA$_{\mathrm{CCC}\text{-}r}$ chart after the t th observation, the initial plotting point Z_0 is defined as

$$Z_0 = E[x]=\frac{r_{\mathrm{EWMA}}}{P_0}. \quad (20)$$

Let L be the width between the center line which is mean and each of the control limits. The upper and lower control limits, h_U and h_L, of the EWMA$_{\mathrm{CCC}\text{-}r}$ chart are obtained as

$$h_U=\frac{r_{\mathrm{EWMA}}}{P_0}+L\frac{\sqrt{r_{\mathrm{EWMA}}(1-P_0)}}{P_0}\sqrt{\frac{\lambda}{(2-\lambda)}}, \quad (21)$$

$$h_L=\frac{r_{\mathrm{EWMA}}}{P_0}-L\frac{\sqrt{r_{\mathrm{EWMA}}(1-P_0)}}{P_0}\sqrt{\frac{\lambda}{(2-\lambda)}}. \quad (22)$$

7. PROPOSAL OF THE SYNTHETIC EWMA CHART

7.1 Settings of Type I Error and Control Limits of The Synthetic EWMA Chart

For setting the control limits of the Synthetic EWMA chart that integrates the EWMA$_{\mathrm{CCC}\text{-}r}$ chart and the CCC-r chart, the actual value of ANOS (Average Number of Observations to Signal) is used instead of that of type I error. The value of ANOS for the EWMA$_{\mathrm{CCC}\text{-}r}$ chart is set to $1/\alpha_{\mathrm{EWMA}}$. For the calculation of ANOS of the EWMA$_{\mathrm{CCC}\text{-}r}$ chart in the Synthetic EWMA chart, the Markov chain approach proposed by Kotani *et al.* (2005) is used. The details on the calculation of ANOS of the Synthetic EWMA chart would be described in subsection 7.4.

Under type I error α_{EWMA} of the EWMA$_{\mathrm{CCC}\text{-}r}$ chart in the Synthetic EWMA chart, for a given value of λ, L is set to actualize ANOS ($=1/\alpha_{\mathrm{EWMA}}$). Substituting the set values of λ and L into equations (21) and (22), the lower and upper control limits, h_L^S and h_U^S, of the EWMA$_{\mathrm{CCC}\text{-}r}$ chart in the Synthetic EWMA chart can be obtained. Under type I error $\alpha_{\mathrm{CCC}\text{-}r}^{\mathrm{EWMA}}$ of the CCC-r chart in the Synthetic EWMA chart, using type I error $\alpha_{\mathrm{CCC}\text{-}r}^{\mathrm{EWMA}}$ of the EWMA$_{\mathrm{CCC}\text{-}r}$ chart in the Synthetic EWMA chart, the lower control limit, LCL, of the CCC-r chart in the Synthetic EWMA chart can be obtained as the solution of the following equation:

$$\sum_{i=r_{\mathrm{CCC}-r}}^{\mathrm{LCL}}\binom{i-1}{r_{\mathrm{CCC}-r}-1}\alpha_{\mathrm{EWMA}}^{r_{\mathrm{CCC}-r}}(1-\alpha_{\mathrm{EWMA}})^{i-r_{\mathrm{CCC}-r}}=\alpha_{\mathrm{CCC}-r}^{\mathrm{EWMA}}. \quad (23)$$

The overall probability of type I error for the Synthetic EWMA chart, α, can be given as

$$\alpha=\alpha_{\mathrm{EWMA}}\times\alpha_{\mathrm{CCC}-r}^{\mathrm{EWMA}}. \quad (24)$$

In this paper, using a parameter w, we set each probability of type I error, α_{EWMA} and $\alpha_{\mathrm{CCC}\text{-}r}^{\mathrm{EWMA}}$, for the EWMA$_{\mathrm{CCC}\text{-}r}$ chart and the CCC-r chart in the Synthetic EWMA chart. In the case that the overall probability of type I error for the Synthetic EWMA chart is set to α, each probability of type I error, α_{EWMA} and $\alpha_{\mathrm{CCC}\text{-}r}^{\mathrm{EWMA}}$, for the EWMA$_{\mathrm{CCC}\text{-}r}$ chart and the CCC-r chart in the Synthetic EWMA chart can be set respectively as follows:

$$\alpha_{\mathrm{EWMA}} = \alpha^{w}, \quad (25)$$

$$\alpha_{\mathrm{CCC}\text{-}r}^{\mathrm{EWMA}} = \alpha^{(1-w)}. \quad (26)$$

7.2 Decision Procedure of The Synthetic EWMA Chart for The Process

According to Figure 2, the decision procedure for the Synthetic EWMA chart is made as follows:

Step 1: In the Synthetic EWMA chart, for the given values of α, r_{EWMA}, $r_{\mathrm{CCC}\text{-}r}$, the lower and upper control limits, h_L^S and h_U^S, of the EWMA$_{\mathrm{CCC}\text{-}r}$ chart and the lower control limit, LCL, of the CCC-r chart are obtained from equations (21)-(23).

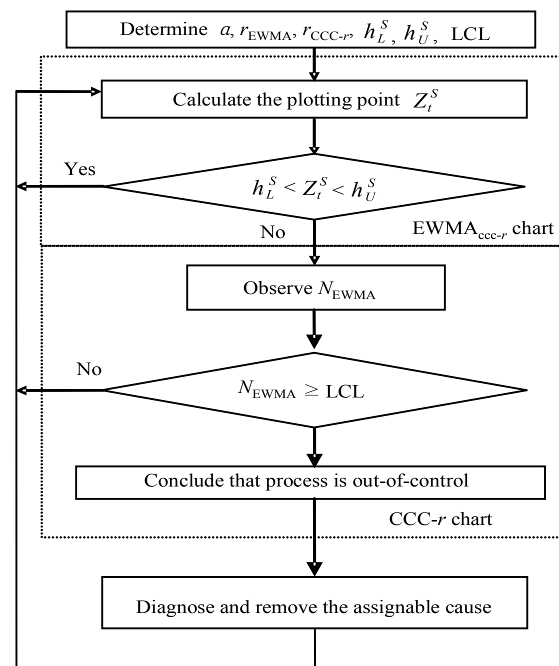

Figure 2. Decision procedure for the Synthetic EWMA chart.

Step 2: For the $\text{EWMA}_{\text{CCC-}r}$ chart in the Synthetic EWMA chart, Z_t^S is initially calculated as the plotting point from equation (18). For Z_t^S, the process is judged, using the lower and upper control limits, h_L^S and h_U^S, of the $\text{EWMA}_{\text{CCC-}r}$ chart in the Synthetic EWMA chart.

Step 3: If Z_t^S exceeds either the lower control limit or the upper control limit, h_L^S and h_U^S, of the $\text{EWMA}_{\text{CCC-}r}$ chart in the Synthetic EWMA chart, Z_t^S is counted as one nonconforming item on the $\text{EWMA}_{\text{CCC-}r}$ chart in the Synthetic EWMA chart.

Step 4: Steps 2 and 3 are repeated until N_{EWMA} is observed on the $\text{EWMA}_{\text{CCC-}r}$ chart in the Synthetic EWMA chart.

Step 5: For N_{EWMA} observed in Step4, the process is furthermore successively judged, using the lower control limit of the CCC-r chart in the Synthetic EWMA chart.

Step 6: If N_{EWMA} exceeds the lower control limit, LCL, of the CCC-r chart in the Synthetic EWMA chart, it would be judged that the process is out-of-control. Otherwise, it would be judged that the process is in-control.

7.3 Calculation of ANOS of the Chart Using Markov Chain Approach

Based on the calculation method to obtain ANOS of the stand-alone $\text{EWMA}_{\text{CCC-}r}$ chart proposed by Kotani *et al.* (2005), the Markov chain approach is used to calculate ANOS of the $\text{EWMA}_{\text{CCC-}r}$ chart in the Synthetic EWMA chart for any shifts in P. The interval between the upper control limit h_U^S and the lower control limit h_L^S obtained from equations (21) and (22) is divided into N subintervals, as shown in Figure 3. The jth subinterval (L_j, U_j) are given as

$$L_j = h_L^S + \frac{(j-1)(h_U^S - h_L^S)}{N}, \tag{27}$$

$$U_j = h_L^S + \frac{j(h_U^S - h_L^S)}{N}. \tag{28}$$

The midpoint m_i of the ith subinterval (L_j, U_j) is given as

$$m_i = h_L^S + \frac{(2i-1)(h_U^S - h_L^S)}{2N}. \tag{29}$$

The (N+1)th state is absorbing and represents the out-of-control region above and below the control limits. This region is considered absorbing because the process is stopped when an out-of-control signal is raised. The ANOS is thus the expected time to absorption of the Markov chain.

The transition probability, P_{ij}, is the probability of

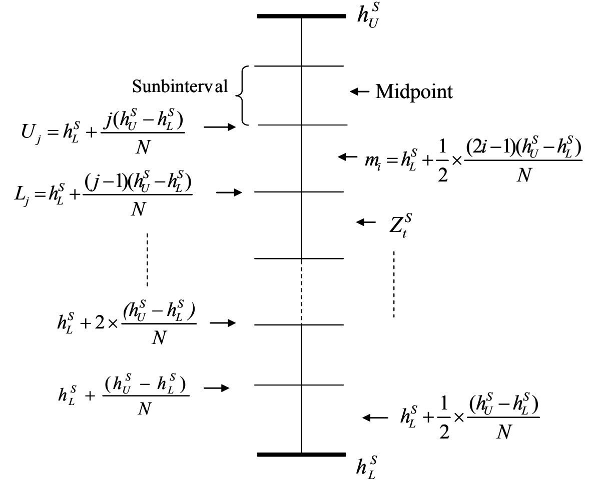

Figure 3. In-control region divided into N subintervals.

moving from state i to state j in one step and is given by

$$P_{ij} = P(L_j < Z_t^S < U_j \mid L_i < Z_{t-1}^S < U_i). \tag{30}$$

This is the probability that Z_t^S is within the boundaries of state j, conditioned on Z_{t-1}^S being equal to the midpoint of state i. This transition probability is obtained as the solution of the following equation:

$$\begin{aligned} P_{ij} &= P(L_j < Z_t^S < U_j \mid Z_{t-1}^S = m_i) \\ &= P(L_j < \lambda x_t + (1-\lambda) Z_{t-1}^S < U_j \mid Z_{t-1}^S = m_i) \\ &= P(L_j < \lambda x_t + (1-\lambda) m_i < U_j) \\ &= P(h_L^S + \frac{(j-1)(h_U^S - h_L^S)}{N} \\ &\quad < \lambda x_t + (1-\lambda)(h_L^S + \frac{1}{2} \times \frac{(2i-1)(h_U^S - h_L^S)}{N}) \\ &\quad < h_L^S + \frac{j(h_U^S - h_L^S)}{N}) \\ &= P(h_L^S + \frac{h_U^S - h_L^S}{2N\lambda}(2(j-1) - (1-\lambda)(2i-1)) \\ &\quad < x_t < h_L^S + \frac{h_U^S - h_L^S}{2N\lambda}(2j - (1-\lambda)(2i-1))). \end{aligned} \tag{31}$$

In general, the left and right sides of equation (31) will not be integer. P_{ij} is calculated based on the distribution function of the negative binomial distribution. For example

$$\begin{aligned} P_{ij} &= P(4.6 < x_t < 6.1) = P(x_t = 5) + P(x_t = 6) \\ &= \binom{5-1}{r-1} P^r (1-P)^{5-r} + \binom{6-1}{r-1} P^r (1-P)^{6-r}. \end{aligned} \tag{32}$$

Define the vector **R** to be

$$\mathbf{R}=[R_1,R_2,\cdots,R_N]^T. \quad (33)$$

Let $\mathbf{Q}$ be the matrix obtained from the transition matrix $\mathbf{P}$ by deleting row $N+1$ and column $N+1$, In other words, $\mathbf{Q}$ is the transition matrix among the in-control states. ANOS vector $\mathbf{R}$ is the solution to the system

$$(\mathbf{I}\text{-}\mathbf{Q})\mathbf{R}=\mathbf{1}, \quad (34)$$

where $\mathbf{I}$ is $N\times N$ identity matrix and $\mathbf{1}$ is a $1\times N$ column vector of ones. ANOS given that $Z_0=\mu_0$ is just the middle entry, that is, the $((N+1)/2)$th entry is the vector $\mathbf{R}$ (We must choose N to be odd so that there is a unique middle value).

Under type I error $\alpha_{\text{EWMA}}{}^w$ of the EWMA$_{\text{CCC-}r}$ chart in the Synthetic EWMA chart, parameter values, λ and L to construct the lower and upper control limits of the EWMA$_{\text{CCC-}r}$ chart in the Synthetic EWMA chart are set so as to actualize ANOS($=(1/\alpha_{\text{EWMA}})^w$) as much as possible.

Using the desired set values of λ and L, the lower and upper control limits, h_L^S and h_U^S, of the the EWMA$_{\text{CCC-}r}$ chart in the Synthetic EWMA chart are obtained from equations (21) and (22). From equation (34), ANOS of the EWMA$_{\text{CCC-}r}$ chart in the Synthetic EWMA chart can be finally calculated.

8. COMPARISON OF THE PERFORMANCE

In order to assess the performance of the detection power of the Synthetic EWMA chart, we compare ANOS (Average Number of Observations to Signal) of the Synthetic EWMA chart with those of the stand-alone EWMA$_{\text{CCC-}r}$ chart and the Synthetic CS chart. Type I error α is set to 0.0027. The in-control population distribution is the negative distribution $NB(r_z, P_0)$ ($z\in$ CS, CCC-r, EWMA) given as $r_z=(2, 5)$ and $P_0=0.001$. We may express the null hypothesis H_0 (the process is the in-control state) and the alternative hypothesis H_1 (the process is the out-of-control state) in a formal manner as

$$H_0: P=P_0,\ H_1: P=P_1=\kappa P_0. \quad (35)$$

In equation (35), in the case that $\kappa=1$, it indicates the in-control state. For $\kappa<1$, it implies that the process changes from the in-control state to the downward direction which indicates the process improvement. Moreover, for $\kappa>1$, it implies that the process changes from the in-control state to the upward direction which indicates the process deterioration.

In order to confirm the detection power of the stand-alone EWMA$_{\text{CCC-}r}$ chart, we first compare ANOS of the stand-alone EWMA$_{\text{CCC-}r}$ chart with that of the stand-alone CS$_{\text{CCC-}r}$ chart(See Kotani *et al.*, 2005). ANOS of the stand-alone CS$_{\text{CCC-}r}$ chart is defined as the expected number of the plotted point x_A required for the stand-alone CS$_{\text{CCC-}r}$ chart to detect the first out-of-control observation. Here, let P_{LCSLcs} denote the lower power of the stand-alone CS$_{\text{CCC-}r}$ chart for P_1. Let P_{UCSLcs} denote the upper power of the stand-alone CS$_{\text{CCC-}r}$ chart for P_1. Under each of the conditions of $NB(r_{\text{CS}}, P_1=\kappa P_0)$ for several values of κ, ANOS of the stand-alone CS$_{\text{CCC-}r}$ chart is obtained as the solution of the following equation (See Ohta and Kusukawa, 2004):

$$\text{ANOS}=\frac{1}{P_{\text{LCSL}_{\text{CS}}}+P_{\text{UCSL}_{\text{CS}}}}, \quad (36)$$

where $$P_{\text{UCSL}_{\text{CS}}}=\left(1-\sum_{i=r_{\text{CS}}}^{\text{UCSL}_{\text{CS}}}\binom{i-1}{r-1}P_1^{r_{\text{CS}}}(1-P_1)^{i-r_{\text{CS}}}\right)^2,$$

$$P_{\text{LCSL}_{\text{CS}}}=\left(\sum_{i=r_{\text{CS}}}^{\text{LCSL}_{\text{CS}}}\binom{i-1}{r-1}P_1^{r_{\text{CS}}}(1-P_1)^{i-r_{\text{CS}}}\right)^2.$$

ANOS of the stand-alone EWMA$_{\text{CCC-}r}$ chart is defined as the expected number of the plotted point Z_t required for the stand-alone EWMA$_{\text{CCC-}r}$ chart to detect the first out-of-control observation. Under each of the conditions of $NB(r_{\text{EWMA}}, P_1=\kappa P_0)$ for several values of κ, ANOS of the stand-alone EWMA$_{\text{CCC-}r}$ chart is obtained as the solutions of equation (34). ANOS of the Synthetic CS chart is defined as the expected number of the plotted point x_A required for the CS$_{\text{CCC-}r}$ chart in the Synthetic CS chart to detect the first out-of-control item. Here, let P_{LCSLs} denote the lower power of the CS$_{\text{CCC-}r}$ chart for P_1 in the Synthetic CS chart. Let P_{UCSLs} denote the upper power of the CS$_{\text{CCC-}r}$ chart for P_1 in the Synthetic CS chart. Under each of the conditions of $NB(r_{\text{CS}}, P_1=\kappa P_0)$ for several values of κ, the lower and upper ANOSs of the Synthetic CS chart are obtained respectively as the solutions of the following equations (See Mishima *et al.,* 2002):

$$\text{Lower ANOS}=\frac{1}{P_{\text{LCSL}_{\text{S}}}}\times\frac{1}{\sum_{i=r_{\text{CCC}-r}}^{\text{LCL}_{\text{LCSL}_\text{S}}}\binom{i-1}{r_{\text{CCC}-r}-1}P_{\text{LCSL}_{\text{S}}}^{r_{\text{CCC}-r}}(1-P_{\text{LCSL}_{\text{S}}})^{i-r_{\text{CCC}-r}}}, \quad (37)$$

$$\text{Upper ANOS}=\frac{1}{P_{\text{UCSL}_{\text{S}}}}\times\frac{1}{\sum_{i=r_{\text{CCC}-r}}^{\text{LCL}_{\text{UCSL}_\text{S}}}\binom{i-1}{r_{\text{CCC}-r}-1}P_{\text{UCSL}_{\text{S}}}^{r_{\text{CCC}-r}}(1-P_{\text{UCSL}_{\text{S}}})^{i-r_{\text{CCC}-r}}}, \quad (38)$$

where the lower and upper powers of the CS$_{\text{CCC-}r}$ chart, P_{LCSLs} and P_{UCSLs}, in the Synthetic CS chart can be obtained respectively as the solutions of the following equations:

$$P_{\text{LCSL}_{\text{S}}}=\left[1-\sum_{i=r_{\text{CS}}}^{\text{UCSL}_{\text{S}}}\binom{i-1}{r_{\text{CS}}-1}P_1^{r_{\text{CS}}}(1-P_1)^{i-r_{\text{CS}}}\right]^2, \quad (39)$$

$$P_{\mathrm{UCSL_S}} = \left[\sum_{i=r_{\mathrm{CS}}}^{\mathrm{LCSL_S}} \binom{i-1}{r_{\mathrm{CS}}-1} P_1^{r_{\mathrm{CS}}} (1-P_1)^{i-r_{\mathrm{CS}}} \right]^2 . \quad (40)$$

ANOS of the Synthetic EWMA chart is defined as the expected number of the plotted point Z_{t-1}^S required for the $\mathrm{EWMA_{CCC\text{-}\mathit{r}}}$ chart in the Synthetic EWMA chart to detect the first out-of-control item. Under each state of $NB(r_{\mathrm{EWMA}}, P_1=\kappa P_0)$ for a given κ, ANOS of the Synthetic EWMA chart can be obtained as the solution of equation (34).

Table 1 shows the lower and upper confirmation control limits and the actual values of type I error α of the stand-alone $\mathrm{CS_{CCC\text{-}\mathit{r}}}$ chart (See Ohta and Kusukawa 2004).

The lower and upper confirmation control limits of the stand-alone $\mathrm{CS_{CCC\text{-}\mathit{r}}}$ chart are obtained respectively as the solutions of equations (7)-(8). Table 2 shows the lower and upper control limits and the actual values of type I error α of the stand-alone $\mathrm{EWMA_{CCC\text{-}\mathit{r}}}$ chart set at parameters λ and L which give the specified value of type I error α and have the high detection powers for any shifts in quality characteristic (See Kotani *et al.*, 2005). The lower and upper control limits of the stand-alone $\mathrm{EWMA_{CCC\text{-}\mathit{r}}}$ chart are obtained respectively as the solutions of equations (21) and (22). Notice that in the stand-alone EWMA chart, a smaller value of λ, say, $\lambda<0.1$ is recommended to detect small shifts in quality characteristic. Through the numerical experiments (See Kotani *et al.,* 2005), it is found that the stand-alone $\mathrm{EWMA_{CCC\text{-}\mathit{r}}}$ chart with $\lambda = 0.06$ has the high detection powers for any shifts in quality characteristics. For $\lambda = 0.06$, a value of L is chosen in the interval $2.5 \le L \le 3.0$ to give the desirable in-control ANOS, in this case, $1/0.0027 \cong 370$. Table 3 shows the lower and upper control limits and the actual values of type I error α of the Synthetic CS chart (See Mishima *et al.,* 2002). The lower and upper control limits of the Synthetic CS chart are obtained respectively as the solutions of equations (9)-(17). Table 4 shows the lower and upper control limits and the actual values of type I error α of the Synthetic EWMA chart set at parameters w, λ and L which actualize the specified value of type I error α and have the high detection powers for any shifts in quality

Table 1. The Confirmation control limits and the actual values of type I error (%) of the stand-alone $\mathrm{CS_{CCC\text{-}\mathit{r}}}$ chart.

$P_0 = 0.001$	Stand-alone $\mathrm{CS_{CCC\text{-}\mathit{r}}}$ Chart		
	$\mathrm{LCSL_{CS}}$	$\mathrm{UCSL_{CS}}$	* Actual values of type I error (%)
$r_{\mathrm{CS}} = 2$	299	5111	0.2695*
$r_{\mathrm{CS}} = 5$	1805	9640	0.2699*

Table 2. The Control limits and the actual values of type I error(%) of the stand-alone $\mathrm{EWMA_{CCC\text{-}\mathit{r}}}$ chart.

$P_0 = 0.001$	Stand-alone $\mathrm{EWMA_{CCC\text{-}\mathit{r}}}$ chart				
	λ	L	h_L	h_U	*Actual values of type I error (%)
$r_{\mathrm{EWMA}} = 2$	0.06	2.563	1363	2637	0.2695*
$r_{\mathrm{EWMA}} = 5$	0.06	2.556	3995	6005	0.2694*

Table 3. The Control limits and the actual values of type I error(%) of the Synthetic CS chart.

$P_0 = 0.001$		Synthetic CS Chart				
$w = 0.5$		$\mathrm{CS_{CCC\text{-}\mathit{r}}}$ Chart		CCC-r Chart		*Actual value of type I error(%)
r_{CS}	$r_{CCC\text{-}r}$	$\mathrm{LCSL_S}$	$\mathrm{UCSL_S}$	$\mathrm{LCL_{LCSL_S}}$	$\mathrm{LCL_{UCSL_S}}$	
2	2	715	3276	14	14	0.2595*
5	5	2856	7130	77	77	0.2595*

Table 4. The Control limits and the actual values of type I error(%) of the Synthetic EWMA chart.

$P_0 = 0.001$			Synthetic EWMA Chart					
			$\mathrm{EWMA_{CCC\text{-}\mathit{r}}}$ Chart				CCC-r Chart	*Actual value of type I error(%)
w	r_{EWMA}	$r_{\mathrm{CCC\text{-}\mathit{r}}}$	λ	L	h_L^S	h_U^S	LCL	
0.8	2	2	0.06	1.989	1506	2494	126	0.2681*
0.75	5	5	0.06	1.840	4269	5731	275	0.2688*

characteristic. The lower and upper control limits of the Synthetic EWMA chart are obtained respectively as the solutions of equations (21)-(26). From Tables 1 - 4, it is illustrated that all charts are designed so as to actualize the specific value of type I error, $\alpha = 0.0027$ as much as possible.

Table 5 shows ANOSs of both the stand-alone EWMA$_{CCC\text{-}r}$ chart and the stand-alone CS$_{CCC\text{-}r}$ chart for $0.5 \le \kappa \le 1.5$. These results are extracted from the numerical experiments investigated by Kotani *et al.* (2005). Table 6 shows ANOSs of the Synthetic EWMA chart and the Synthetic CS chart for $0.5 \le \kappa \le 1.5$. The results of ANOS of the Synthetic CS chart for $0.5 \le \kappa \le 1.5$ are extracted from the numerical experiments investigated by Mishima *et al.* (2002). Here, the closer to 0 the value of ANOS of the chart is, the more sensitive the detection for any shifts in quality characteristics from the in-control state is, while the closer to ∞ the value of ANOS of the chart, the less sensitive the detection for any shifts in quality characteristics from the in-control state is. Notice that the stand-alone CS$_{CCC\text{-}r}$ chart and the Synthetic CS chart are designed to monitor quality characteristics in real-time, whereas the stand-alone EWMA$_{CCC\text{-}r}$ chart and the Synthetic EWMA chart consider combining the quality characteristics monitored in the past with one monitored in real-time.It is demonstrated from Table 5 that ANOSs of the stand-alone EWMA$_{CCC\text{-}r}$ chart are smaller than those of the stand-alone CS$_{CCC\text{-}r}$ chart for the upward shifts in P (case that κ >1) from the in-control state and the downward shifts in P (case that κ <1) from the in-control state. From the results, it can be seen that the stand-alone EWMA$_{CCC\text{-}r}$ chart is more sensitive to detect any shifts in P from the in-control state than the stand-alone CS$_{CCC\text{-}r}$ chart. It is evident from Table 6 that for r_z (z$\in$CS, CCC-r, EWMA) = (2, 5), ANOSs of the Synthetic EWMA chart are smaller than those of the stand-alone EWMA$_{CCC\text{-}r}$ chart for the small and moderate shifts in P from the in-control state to the upward direction (the cases that κ >1) and the small and moderate shifts in P from the in-control state to the downward direction (the cases that κ <1). From the results, it is demonstrated that the Synthetic EWMA chart is more sensitive to detect any shifts in P from the in-control state than the stand-alone EWMA$_{CCC\text{-}r}$ chart. It is evident from Table 6 that for r_z (z$\in$CS, CCC-r, EWMA) = 5, there isn't so much of a difference between ANOSs of the Synthetic EWMA chart and those of the Synthetic CS chart for $0.5 \le \kappa \le 1.5$. For r_z (z$\in$CS, CCC-r, EWMA) = 5 and $0.9 \le \kappa \le 1.1$ which indicates the small shifts in P from the in-control state to both the upward and downward directions, ANOSs of the Synthetic EWMA chart are reduced highly, compared to the stand-alone CS$_{CCC\text{-}r}$ chart, the stand-alone EWMA$_{CCC\text{-}r}$ chart and the Synthetic CS chart.

It is illustrated from Table 6 that even for r_z (z$\in$CS, CCC-r, EWMA) = 2, ANOSs of the Synthetic EWMA chart are smaller than those of the Synthetic CS chart for the small and moderate shifts to the upward direction in P (the cases that $1 < \kappa \le 1.5$) and the small shifts in P from the in-control state to the downward direction (cases that $0.7 \le \kappa < 1$). From the results, it can be seen that even for r_z (z$\in$CS, CCC-r, EWMA) = 2, the Syn-

Table 5. Comparison of ANOSs of the stand-alone CS$_{CCC\text{-}r}$ chart with those of the stand-alone EWMA$_{CCC\text{-}r}$ chart.

*: Actual value of type I error (%)		κ										
		0.5	0.6	0.7	0.8	0.9	1.0	1.1	1.2	1.3	1.4	1.5
CS$_{CCC\text{-}r}$ Chart $r_{CS} = 2$		13	28	60	127	246	0.2695*	406	355	285	224	178
EWMA$_{CCC\text{-}r}$ Chart $r_{EWMA} = 2$	$\lambda = 0.06$, $L = 2.563$	**8**	**12**	**20**	**39**	**104**	0.2695*	**366**	**138**	**70**	**45**	**34**
CS$_{CCC\text{-}r}$ Chart $r_{CS} = 5$		**4**	10	26	71	197	0.2699*	332	207	125	79	52
EWMA$_{CCC\text{-}r}$ Chart $r_{EWMA} = 5$	$\lambda = 0.06$, $L = 2.556$	5	**7**	**11**	**22**	**65**	0.2694*	**140**	**48**	**27**	**19**	**15**

Table 6. Comparison of ANOSs of the Synthetic CS chart with those of the Synthetic EWMA chart.

* : Actual value of type I error (%)	w \ κ	0.5	0.6	0.7	0.8	0.9	1.0	1.1	1.2	1.3	1.4	1.5
Synthetic CS Chart $r_{CS} = r_{CCC\text{-}r} = 2$	0.5	4	8	19	56	179	0.2595*	313	170	94	56	35
Synthetic EWMA Chart $r_{EWMA} = r_{CCC\text{-}r} = 2$	0.8	6	9	**14**	**27**	**83**	0.2681*	**252**	**79**	**39**	**26**	**21**
Synthetic CS Chart $r_{CS} = r_{CCC\text{-}r} = 5$	0.5	2	3	5	10	45	0.2616*	93	24	11	7	6
Synthetic EWMA Chart $r_{EWMA} = r_{CCC\text{-}r} = 5$	0.75	3	5	8	14	**37**	0.2688*	**71**	**24**	16	12	10

thetic EWMA chart is more sensitive to detect the small shifts in P from the in-control state than the Synthetic CS chart to both the upward and downward directions. It implies that even with less number of inspection items from the process, the Synthetic EWMA chart can enhance the detection power for any shifts as well as the small and moderate shifts from the in-control state to both the upward and downward directions. Therefore, it is verified that it is the most adequate to use the Synthetic EWMA chart in the high-yield process as the alternative chart to detect sensitively any shifts in quality characteristics from the in-control state with a small size of inspection items observed from the process monitored.

From the comparison of ANOS performances of each control chart, our purpose has been successfully achieved.

9. CONCLUSIONS

The manufacturing processes, especially in the electronic industries, had been automated with the aid of computers and the modern technologies. Moreover, in the real field, the fundamental aim of the monitoring and improving actions of the process quality was always to realize the zero-defects processes. From this viewpoint, in this paper, we focused on enhancing the detention power for especially the small shifts in the fraction defective to both the upward and downward directions which the process deterioration and the process improvement in the high-yield processes. Concretely, we presented a Synthetic EWMA chart that was an integration of the $\text{EWMA}_{\text{CCC-}r}$ chart and the CCC-r chart to enhance the detection power for the small or moderate shifts in the process fraction defectives from the in-control state to both the upward and downward directions in the high-yield processes seen in the manufacturing environment of today. The Synthetic EWMA chart was constructed by applying the designing method of the Synthetic CS chart to the stand-alone $\text{EWMA}_{\text{CCC-}r}$ chart which considered combining the quality characteristics monitored in the past with one monitored in real-time. Based on the calculation method to obtain ANOS (Average Number of Observations to Signal) of the stand-alone $\text{EWMA}_{\text{CCC-}r}$ chart, the Markov chain approach was used to calculate ANOS of the Synthetic EWMA chart for any shifts in the process fraction defectives from the in-control state. Comparing ANOS of the Synthetic EWMA chart with those of the stand-alone $\text{EWMA}_{\text{CCC-}r}$ chart and the Synthetic CS chart, it was verified that the Synthetic EWMA chart was the most sensitive chart to detect the small or moderate shifts in the process fraction defectives to both the upward and downward directions in the high-yield processes among the stand-alone $\text{EWMA}_{\text{CCC-}r}$ chart and the Synthetic CS chart, even when the number of nonconforming item observed before a point is plotted on the chart, r, was set to a small value. As r increases, there was not so much of a difference between ANOSs of the Synthetic EWMA chart and those of the Synthetic CS chart for the moderate shifts in the process fraction defective from the in-control state. From both the aspects of the operational cost of the chart and the detection power of the chart, it was the most adequate to use the Synthetic EWMA chart in the high-yield processes as the alternative chart. The proposed process monitoring technique could be implemented with the help of the on-line computers and the modern inspection equipment in the automated manufacturing environment in order to enhance the detection powers for the small shifts in the process fraction defectives with a small size of the inspection items observed from the process monitored.

As r increases, the Synthetic EWMA chart is more and more sensitive to detect the small or moderate shifts in the process fraction defectives to both the upward and downward directions, while more and more observations are required to obtain a plotting point on the chart. From the trade-off problem, it is necessary to determine the economical designing parameters such as the number of nonconforming item observed before a point is plotted on the chart, the sampling (inspection) interval and the lower and upper control limits of the Synthetic EWMA chart. The issue of an economical design of the Synthetic EWMA chart will be left for future research.

REFERENCES

Borror, C. M., Champ, C. W., and Rigdon, S. E. (1998), Poisson EWMA Control Charts, *Journal of Quality Technology*, **30**, 352-361.

Crowder, S. V. (1987), A Simple Method for Studying Run Length Distributions of Exponentially Weighted Moving Average Control Charts, *Technometrics*, **29**, 401-407.

Domangue, R. and Patch, S. C. (1991), Some Omnibus Exponentially Weighted Moving Average Statistical Process Monitoring Schemes, *Technometrics*, **33**, 299-313.

Gan, F. F. (1990), Monitoring Poisson Observations Using Modified Exponentially Weighted Moving Average Control Charts, *Communications in Statistics-Simulation and Computation*, **19**, 103-124.

Gan, F. F. (2002), Monitoring Poisson Observations Using Modified Exponentially Weighted Moving Average Control Charts, *Communications in Statistics-Simulation and Computation*, **19**, 103-124.

Kotani, T., Kusukawa, E., and Ohta, H. (2005), Exponentially Weighted Moving Average Chart for High-Yield Processes, *Industrial Engineering and Management Systems*, **4**, 75-81.

Kusukawa, E. and Ohta, H. (2003), A Modified Synthetic Chart for High-Yield Processes. *Proceedings of the 17th International Conference on Production*

Research, *Blacksburg*, *VA*, 18 pages total (CD-ROM publications).

Lucas, J. M. and Saccucci, M. S. (1990), Exponentially Weighted Moving Average Control Schemes: Properties and Enhancements, *Technometrics*, **32**, 1-12.

Mishima, N. Kusukawa, E., and Ohta, H. (2002), A Synthetic chart for Very-High-Yield Processes, *Proceedings of Seventh International Pacific Conference on Manufacturing & Management*, *Bangkok, Thailand,* 799-80.

Montgomery, D. C. (2001), *Introduction to Statistical Quality Control*, 4th ed., John Wily and Sons, New York, NY.

Ng, C. H. and Case, K. E. (1989), Development and Evaluation of Control Charts Using Exponentially Weighted Moving Averages, *Journal of Quality Technology*, **21**, 242-250.

Ohta, H. and Kusukawa, E. (2004), *An Application of Confirmation Sample Control Chart to the High-Yield Processes and Its Economic Design. In H -J. Lenz and P -TH. Wilrich (ed)*, *Frontiers in Statistical Quality Control 7*, *(New York: Physica-Verlag)*, chapter 2, 101-118.

Reynolds, M. R. Jr. (1996), Shewhart and EWMA Variable Sampling Interval Control Charts with Sampling at fixed times, *Journal of Quality Technology*, **28**, 199-212.

Reynolds, M. R. Jr. and Stoumbos, Z. G. (1999), A Cusum Chart for Monitoring a Proportion When Inspection Continuously, *Journal of Quality Technology*, **31**, 87-108.

Roberts, S. W. (1959), Control Chart Tests Based on Geometric Moving Averages, *Technometrics*, **1**, 239-250.

Roberts, S. W. (1966), A Comparison of Some Control Chart Procedures, *Technometrics*, **8**, 411-430.

Steiner, S. H. (1998), Grouped Data Exponentially Weighted Moving Average Control Chart, *Applied Statistics*, **47**, 203-216.

Steiner, S. H. (1999), Confirming Sample Control Charts, *International Journal of Production Research*, **37**, 737-748.

Xie, M., Goh, T. N., and Lu, X. S. (1998), Computer–Aided Statistical Monitoring of Automated Manufacturing Process, *Journal of Computers and Industrial Engineering*, **35**, 189-192.

Wu, Z. and Spedding, T. A. (2000), A Synthetic Control Chart for Detecting Small Shifts in the Process Mean, *Journal of Quality Technology*, **32**, 32-38.